Self-consistent transport simulations of COMPASS operation with NBI

Jakub Urban[1], Michal Stránský[1], Vladimír Fuchs[1], Irina Voitsekhovitch[2] and Martin Valovič[2]

[1] Institute of Plasma Physics AS CR, v.v.i., Association EURATOM/IPP.CR, Prague, Czech Republic

[2] EURATOM/UKAEA Fusion Association, Culham Science Centre, Abingdon, Oxon OX14 3DB, UK

E-mail: urban@ipp.cas.cz

Abstract. The COMPASS tokamak, a mid-sized flexible device with ITER-like shape, which can operate in H-mode, is starting its re-established operation at the Institute of Plasma Physics in Prague. A new 600 kW, 40 keV neutral beam injection (NBI) system is foreseen as a major upgrade. Reported here are predictive simulations with the ASTRA transport code, in which the FAFNER Monte-Carlo NBI code is, for the first time, self-consistently integrated. These simulations are carried out for several typical COMPASS scenarios with differing magnetic fields, plasma currents and shapes. We compare Ohmic scenarios with NBI-heated scenarios and show that NBI is able to significantly improve the plasma performance, particularly to attain $T_\mathrm{i} \cong T_\mathrm{e}$, which is the primary goal of the NBI system. The NBI performance is discussed in detail. The chosen energy of 40 keV is shown to be in many aspects optimum. Simulations also predict substantial losses—orbit losses are pronounced for counter-current injection and charge-exchange losses caused by beam-halo neutrals are raised due to high NBI particle input.

PACS numbers: 52.55.Fa, 52.50.Gj, 52.65.-y

1. Introduction

The COMPASS (COMPact ASSembly) tokamak ($R_0 = 0.56$ m, $a = 0.2$ m, $B_0 = 0.8 - 2.1$ T, $I_\mathrm{p} < 350$ kA) was recently transported from UKAEA Culham to the Institute of Plasma Physics Prague [1]. The first plasma was obtained in 2008 and the tokamak is presently operational. The COMPASS device, designed as a flexible tokamak in the 1980s, has an ITER-like plasma shape and can operate in the H-mode confinement regime. With the anticipated heating and current drive systems, such as the lower hybrid (LH) and the neutral beam injection (NBI), it should be possible to access plasma parameters relevant in many respects to ITER. A particularly important upgrade in COMPASS is the new NBI system, which is expected to significantly increase

the plasma performance in COMPASS, particularly to attain plasmas with the ion temperature comparable to the electron temperature.

The main goal of this paper is to estimate the performance of the COMPASS tokamak with NBI. Plasma equilibria with NBI and LH were first investigated using the magnetic equilibrium – current drive code ACCOME [2, 3, 4]. Reported here are results from the plasma transport code ASTRA [5] and the IPP Garching NBI code FAFNER [6, 7], which has been, for the first time, self-consistently integrated in ASTRA. We present selected results of these simulations at typical foreseen operating conditions: $I_\mathrm{p} = 150 - 250$ kA and $B_0 = 1.2 - 2.1$ T.

In section 2 we describe the simulation methods and the parameters used for COMPASS. Section 3 describes the NBI system and shows the simulation results from FAFNER. Section 4 deals with the self-consistent ASTRA-FAFNER simulations. Finally, section 5 gives our conclusions.

2. Simulation methods and setup

The common basis for the simulations reported here is the transport code ASTRA [5]. The macroscopic equilibrium parameters have been setup according to ACCOME results [8, 4], particularly the plasma major and minor radius, elongation, triangularity (therefore the last closed flux surface is fully determined) and the total plasma current. The electron density profiles and the effective ion charge Z_eff were fixed in the simulations. Two plasma shapes are used in our simulations: SND (single-null-divertor, elongation $\kappa = 1.53$, triangularity $\delta = 0.4$) and SNT (single-null-divertor with higher triangularity, $\kappa = 1.75$, $\delta = 0.47$). Two values of the on-axis toroidal magnetic field are used: $B_0 = 1.2$ T (plasma current $I_\mathrm{p} = 175$ kA, abbreviated SND1, SNT1 in the text) and $B_0 = 2.1$ T (plasma current $I_\mathrm{p} = 250$ kA, abbreviated SND2, SNT2 in the text). These parameters of the configurations are also given in section 4.1, Table 1.

A major feature added to ASTRA is a self-consistent integration of the Monte-Carlo NBI code FAFNER [6]. This 3D code calculates, using a Monte-Carlo technique, the ionization of the NBI neutrals and the subsequent fast ions behaviour in the plasma, accounting for shine-through, charge-exchange and orbit losses. The principal outcome of such calculations are profiles of absorbed power densities and driven current densities. The FAFNER code was previously used for COMPASS NBI simulations [7] as a standalone module. Presently, FAFNER is integrated self-consistently into ASTRA. The 2D equilibrium calculated in ASTRA, i.e., the poloidal flux function $\psi(R, Z)$, the toroidal flux function $F(\psi) = RB_\phi$, the plasma profiles $n_\mathrm{e}(\psi)$, $T_\mathrm{e}(\psi)$, $T_\mathrm{i}(\psi)$ and Z_eff, are transferred to FAFNER. In turn, FAFNER outputs, particularly the power densities absorbed by electrons and ions and the driven current density, are then input into ASTRA. A typical single FAFNER run takes several minutes on a single CPU; therefore, it would be extremely slow to run FAFNER for every single ASTRA time step, which is on the order of a millisecond. As we are interested in a steady state and not in the temporal evolution, we can call FAFNER after rather long time steps,

providing that ASTRA reaches a steady state between the calls. An equilibrium should be established after several iterations when neither FAFNER nor ASTRA results are changing considerably.

3. The Neutral Beam Injection (NBI)

3.1. NBI System Design

A flexible NBI system is planned for COMPASS, consisting of two injectors with particle energy 40 keV and 300 kW output power, delivering a total of 600 kW to the plasma (neglecting losses in the beam duct). Inclination of the NB injection angle from the tangential direction was originally foreseen in the range of 0 – 4° (0 – 50 mm) to investigate off-axis heating. Recent calculations of the beam duct throughput, however, indicate that an updated design is required to avoid beam blocking. This design involves significant widening of the beam duct, which does not allow any inclination. Details of the original NBI system design can be found in [7]. The injectors will be connected to tangential ports, with the possibility of switching one of the injectors from co-current direction to counter-current direction with the aim of enabling non-rotating, NBI-heated plasmas. The basic configurations are dual co-injection (Fig. 1a) and balanced (co+counter) injection (Fig. 1b). We also study the possibilities of single co- and counter-injection, where only a single injector is used. Dual counter-injection because of excessive associated ion orbit losses is not a viable option here.

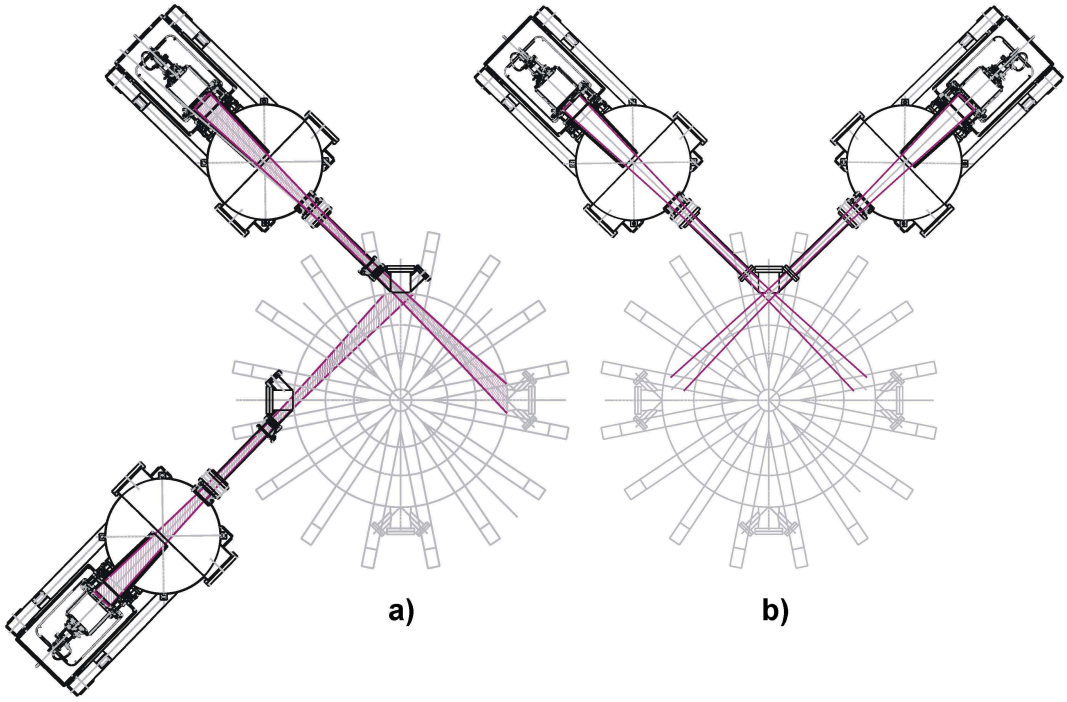

Figure 1. Planned neutral beam injectors for a) dual co-injection and b) balanced injection (from [7]).

3.2. NBI simulation results

Intensive computations have been performed to simulate NBI behaviour on COMPASS using the Monte-Carlo code FAFNER within ASTRA. The SND and SNT equilibria with low and high magnetic fields, described above, are applied for the simulations. Analyzed in this section are results from the last iteration of the ASTRA-FAFNER simulations described in section 4.2.

Energy balance results are shown in Fig. 2 for 1.2 T and 2.1 T SND equilibria and various injection scenarios. Results for SNT equilibria (not shown here) do not significantly differ from the SND results. There are three major loss-channels present. "Shine-through", i.e., the portion of neutrals not ionized in the plasma, scales moderately with the central density. For the higher density cases, with the central density $n_\mathrm{e} = 5 \times 10^{19}$ m^{-3}, the shine-through losses drop to approximately 2 %. The shine-through is hence very low in our case. Very important are orbit losses, i.e., losses caused by those beam ions, whose orbits cross the plasma boundary, and which therefore do not deliver their energy to the confined plasma. For the low magnetic field equilibrium SND1, the orbit losses are predicted to be around 15 % for single co-injection and 17 % for dual co-injection. For the high field SND2 equilibrium, the orbit losses drop to 8 % for single and 11 % for double co-injection. However, these losses become very pronounced for counter-injection, where they can be as high as 50 %, depending on the equilibrium and the density (see Fig. 2). As a consequence, counter-injection is considerably less efficient than co-injection. For the balanced injection, moderate orbit losses of 11 – 26 % (depending on the density) are predicted for SND2, while rather high orbit losses of 26 – 36 % are predicted for SND1. Charge-exchange losses, caused by neutrals coming from the walls, are also included. The neutral density profile is, however, not well known and therefore rather low neutral density of $\sim 3 \times 10^{17}$ m^{-3} at the LCFS and an exponential decay to the centre was prescribed. Ten times higher neutral densities with a longer decay length did not have any substantial effect on the calculated charge-exchange losses and hence we kept the lower value, effectively almost neglecting charge-exchange losses at the edge. These losses would anyway have only a minor effect on our results.

In the previous studies [7, 8], we considered only a single 300 kW injector and presumed that the results can be simply doubled to obtain realistic estimates for the whole NBI system performance. This is, however, not true because of the so-called beam-halo effect. 40 keV neutrals will be dominantly ionized by the charge-exchange mechanism, thus creating neutrals (with Maxwell's distribution with the temperature equal to the ion temperature) along the beam path. These neutrals can again interact with the fast beam ions. Another charge-exchange collision may occur, after which a fast ion becomes a fast neutral and can escape the plasma. This effect is studied with the Monte-Carlo technique described in [9] and implemented in FAFNER. The beam-halo neutral density n_0^h obviously grows with the number of the injected neutrals. The fast ions slowing down time constant is proportional to $T_\mathrm{e}^{3/2}/n_\mathrm{e}$ [10] while the

charge-exchange collision frequency is proportional to $\sigma_{\rm ch} n_0^{\rm h}$, where $\sigma_{\rm ch}$ is the relevant charge-exchange cross section. The severity of charge-exchange losses caused by the beam-halo neutrals is mainly determined by the ratio $n_0^{\rm h}/n_{\rm e}$. This dependence also indicates that higher electron temperatures, predicted for the 2.1 T equilibria with 250 kA plasma current, cause higher charge-exchange losses, as can be seen in Fig. 2. On the other hand, higher electron temperature induces higher critical energy, at which the fast ions begin to deposit most of their energy to ions during the slowing down process. This is favourable for attaining plasmas with $T_{\rm i} \cong T_{\rm e}$. Higher density acts positively on NBI performance, except for current drive efficiency, by decreasing the shine-through and the charge-exchange losses.

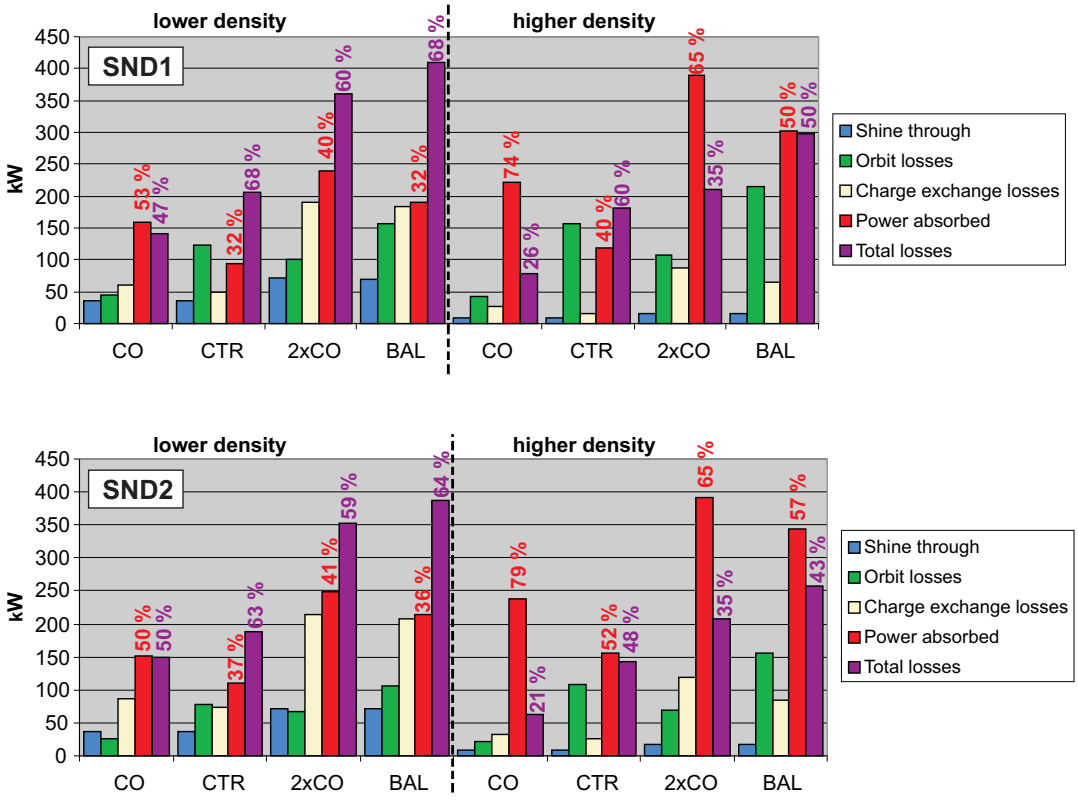

Figure 2. NBI performance of the studied NBI scenarios, simulated with SND1 (top) and SND2 (bottom) COMPASS equilibria. Plotted are configurations with lower (3×10^{19} m^{-3}) and higher (5×10^{19} m^{-3}) central electron densities. CO denotes co-injection with respect to the plasma current direction, CTR denotes counter-injection, 2×CO stands for the dual co-injection setup and BAL for the balanced injection setup.

The current drive predictions are shown in Fig. 3. For the low field equilibria with $T_{\rm e} = 1 - 1.2$ keV, the maximum current is 36 kA with dual co-injection, constituting 20 % of the total plasma current. For the high field equilibria with $T_{\rm e} = 1.5 - 1.8$ keV, the driven current is higher, with maximum of 44 kA (in the lower density case). The percentage of the total plasma current is 18 % in this case. There are generally no major differences in the NBI current drive performance for the studied SND and SNT equilibria.

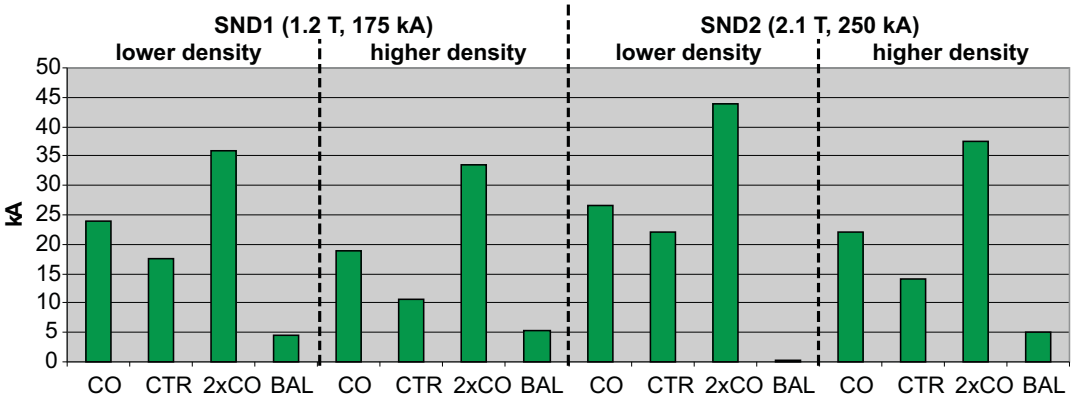

Figure 3. Total NBI driven current for the cases in Fig. 2.

A more detailed analysis can be performed examining the deposition profiles of the dual co-injection and balanced injection scenarios, plotted in Fig. 4. First we see a well-centralized deposition, corresponding to the tangential injection setup. (The tangency radius equals the tokamak major radius.) The total deposited power densities reach 6.5 MW/m^3 and 10 MW/m^3 during dual co-injection for the low field and for the high field cases, respectively. Peak current densities are 2.7 MA/m^2 and 4.7 MA/m^2 in these cases. The distribution of the deposited energy between electrons and ions (indicated in Fig. 4 and 5) does not significantly depend on the equilibrium. Ions absorb a greater part of the power in all the studied scenarios (with a single exception of counter injection, SND1, higher-density). Particularly for dual co-injection, higher density, it is 52 % for SND1 and 60 % for SND2.

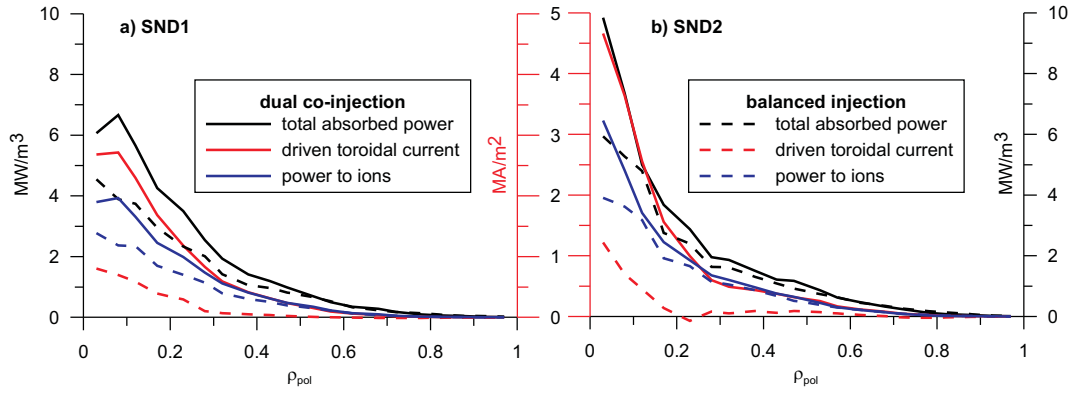

Figure 4. Power deposition and current drive profiles for a) SND1 and b) SND2 equilibrium, calculated for the dual co-injection and the balanced injection scenarios, $n_e = 5 \times 10^{19}$ m^{-3}.

3.3. Optimization of the beam particle energy

A possible way of further optimizing the NBI performance is to use a different particle energy. Results obtained with FAFNER for various energies, SND1 and SND2 equilibria

and $n_e = 5 \times 10^{19}$ m^{-3}, are presented in Fig. 5. Increasing the energy to 60 keV leads generally to higher losses because of the higher shine-through and a longer thermalization time. Moreover, a larger portion of the power is deposited on electrons. For the same reasons, the overall performance is slightly better for 30 keV compared to 40 keV. The deposition profiles are very similar for central electron densities up to 8×10^{19} m^{-3}. Larger densities cause 30 keV beams to deposit the power closer to the plasma edge. A disadvantage of using 30 keV would be a 1.3 times higher particle current necessary to obtain 300 kW of power. This represents a higher risk of the beam duct blocking.

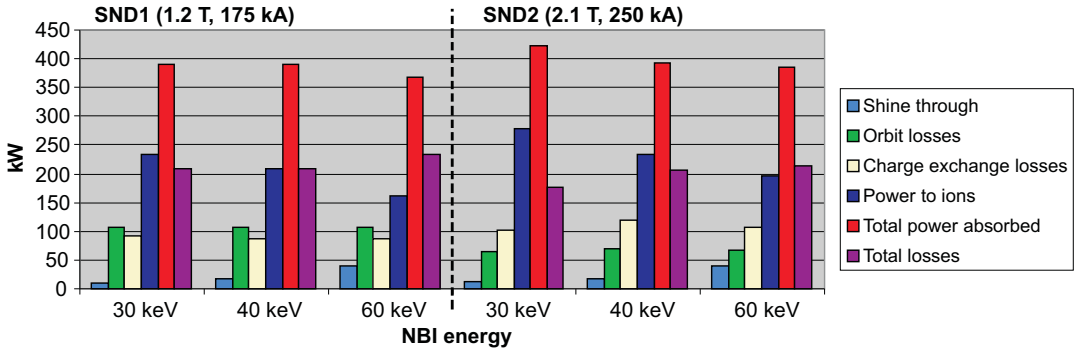

Figure 5. Dual-injection NBI performance for 30 keV, 40 keV and 60 keV energies, SND equilibria described above, $n_e = 5 \times 10^{19}$ m^{-3}.

In addition to tangential injection, optimized for heating performance, we also consider normal (radial) injection for possible diagnostic applications. The same port can be used in this case, with the beam injected through the wider flange, which is pointing radially. Results presented in Fig. 6 were obtained for the SND2 equilibrium with a single 300 kW NBI, various densities and particle energies. The shine-through represents a serious danger in this case. For 50 kW shine-through, the carbon inner wall load is around 17 MW/m^2. This is comparable to divertor loads. Orbit losses will be deposited mainly on the divertor plates. Charge-exchange losses, where the power is carried by fast neutrals, will be more or less uniformly deposited on the walls around the toroidal position of the injection. The best energy for the normal injection is certainly 20 keV because of the significantly lower losses, especially the shine-through. A system which allows decreasing the particle energy to 20 keV is thus desirable here. The output power would probably decrease with lower energy. Even this decreased power should be, however, sufficient for most of beam diagnostics.

4. ASTRA – FAFNER simulations

Predictive simulations of COMPASS performance with NBI are highly desirable. This modelling is performed here using the ASTRA (Automated System for Transport Analysis) [5] transport code. The simulations are performed for a few basic COMPASS single-null divertor operation scenarios at low and high triangularity, SND and SNT,

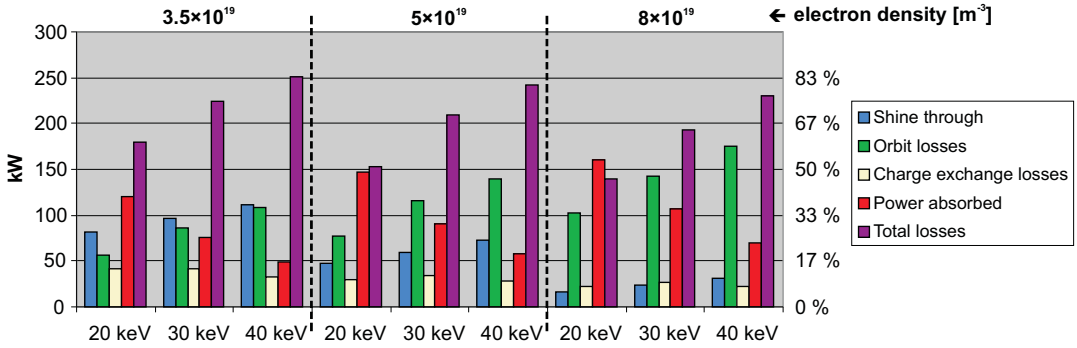

Figure 6. Performance of a single 300 kW NBI injected normally (radially), SND2 2.1 T equilibrium, electron temperature 1.5 keV and central electron densities 3.5×10^{19} m^{-3}, 5×10^{19} m^{-3}, 8×10^{19} m^{-3}.

respectively, and at lower and higher magnetic fields and currents, as specified above in section 2. The higher triangularity scenarios SNT1,2 provide access to higher confinement and improved stability.

The electron thermal transport model used for simulating the COMPASS tokamak is the mixed Bohm-gyroBohm model [11] recalibrated for matching the measured central electron temperature in previous COMPASS experiments [12]. The ion thermal transport was modelled using twice the anomalous heat diffusivity [11], as suggested in [13]. The electron and ion neoclassical diffusivity added to the anomalous transport has been simulated with NCLASS [14]. With these assumptions on transport models, a good agreement for the measured diamagnetic energy in experiments [12] has been obtained.

The particle transport was not simulated and instead the electron density profile is prescribed as in Ref. [12]:

$$n_{\mathrm{e}} = (n_0 - n_{\mathrm{b}}) \left[1 - (r/a)^2\right]^{0.5} + n_{\mathrm{b}}.$$

Here, r is the radius in the tokamak mid-plane, and a is its minor radius; the central electron density was set to $n_0 = 5 \times 10^{19}$ m^{-3} and the edge density to $n_{\mathrm{b}} = 0.1 \times 10^{19}$ m^{-3}. The main ion species in plasma was D^+, and a carbon impurity was included. The ion species density profiles were calculated from a prescribed Z_{eff} profile.

In our modelling, NBI power deposition was calculated by the FAFNER code [6], which we incorporated into ASTRA, thereby making possible self-consistent transport simulations with NBI heating.

4.1. Ohmic heating reference results

For reference, ohmic heating simulations were performed, and the electron and ion temperatures profiles are plotted in Fig. 7. The ASTRA simulations show a slightly worse confinement in the higher triangularity (SNT) cases than in the corresponding SND cases. The beneficial effect of the higher triangularity seems to be overshadowed by the extreme sensitivity of the transport coefficients to the value of q^2. Since the central

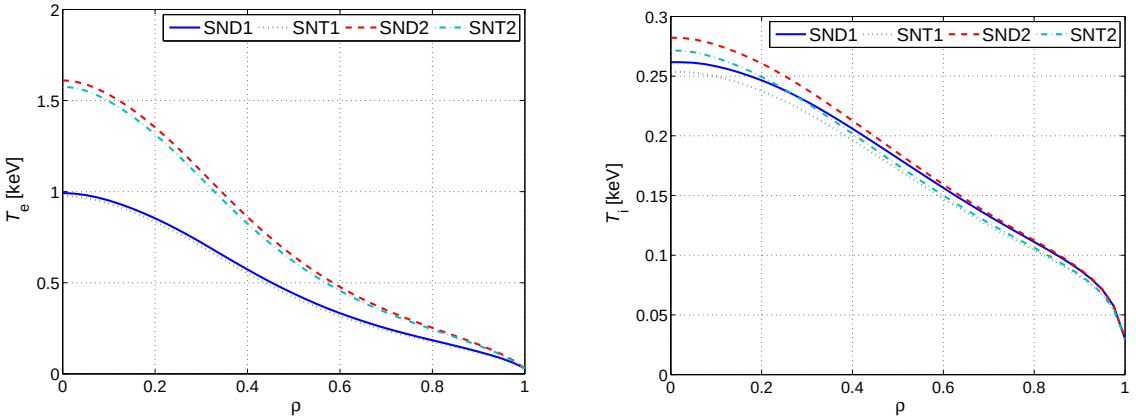

Figure 7. The electron (left) and the ion (right) temperature profiles in the ohmic heating case. On the axis, the temperature attained from lowest to highest are ordered: SNT1, SND1, SNT2 and SND2.

values of q are smaller in the SND than in the SNT equilibria, the SND cases reach higher central temperatures. An issue not considered here are possibly different electron and ion boundary temperature conditions in the SND and SNT operation modes. Having here prescribed the same boundary temperatures in SND and SNT, we effectively simulated L-mode plasmas. It is experimentally observed that higher triangularity regimes may have a larger pedestal due to improved stability giving an overall better confinement, but H-mode physics and sophisticated edge plasma physics were not included in the simulations so far, so the SNT cases end up worse.

The following Table 1 summarizes the case parameters and ohmic simulation results. The magnetic equilibria parameters such as the elongation and triangularity are determined from ACCOME [8] and depend on the basic equilibrium setup as a function of the toroidal magnetic field, the plasma current, and the external poloidal field coil system.

Table 1. Ohmic case heating parameters and results including the plasma current (I_p), on-axis toroidal magnetic field (B_0), elongation (κ), triangularity (δ), central electron (T_e0) and ion (T_i0) temperatures, ohmic heating power (P_OH) and energy confinement time (τ_E).

Case	I_p [kA]	B_0 [T]	κ	δ	T_e0 [keV]	T_i0 [keV]	P_OH [kW]	τ_E [ms]
SND1	175	1.2	1.53	0.4	0.99	0.26	184	17
SNT1	175	1.2	1.75	0.47	0.98	0.25	188	15
SND2	250	2.1	1.53	0.4	1.61	0.28	253	13
SNT2	250	2.1	1.75	0.47	1.58	0.27	257	12

4.2. NBI-heated plasma

Several issues had to be addressed for the ASTRA simulations. One of them is the rather uncertain ion transport model mentioned above, which has not been tested in the experiments described in [12], but matches the thermal ion transport in L-mode regimes on other tokamaks. Another is the sawtooth modelling. This was not a problem in the ohmic case because low values of q near the magnetic axis are handled by an ASTRA MHD resistivity function, effectively reducing the central current and not allowing q_0 to drop below 1. However, changing the resistivity doesn't affect the non-inductively driven current, so this function cannot regulate q_0 back up to values close to 1 when the central non-inductively driven current is significant compared to ohmic. Similarly, ASTRA provides MHD routines that modify heat diffusivity coefficients when $q < 1$, partially handling the problem. A possible way of avoiding the problem with sawtoothing is to limit the central non-inductively driven current by aiming the NBI more off-axis. This, however, results in low central ion temperatures.

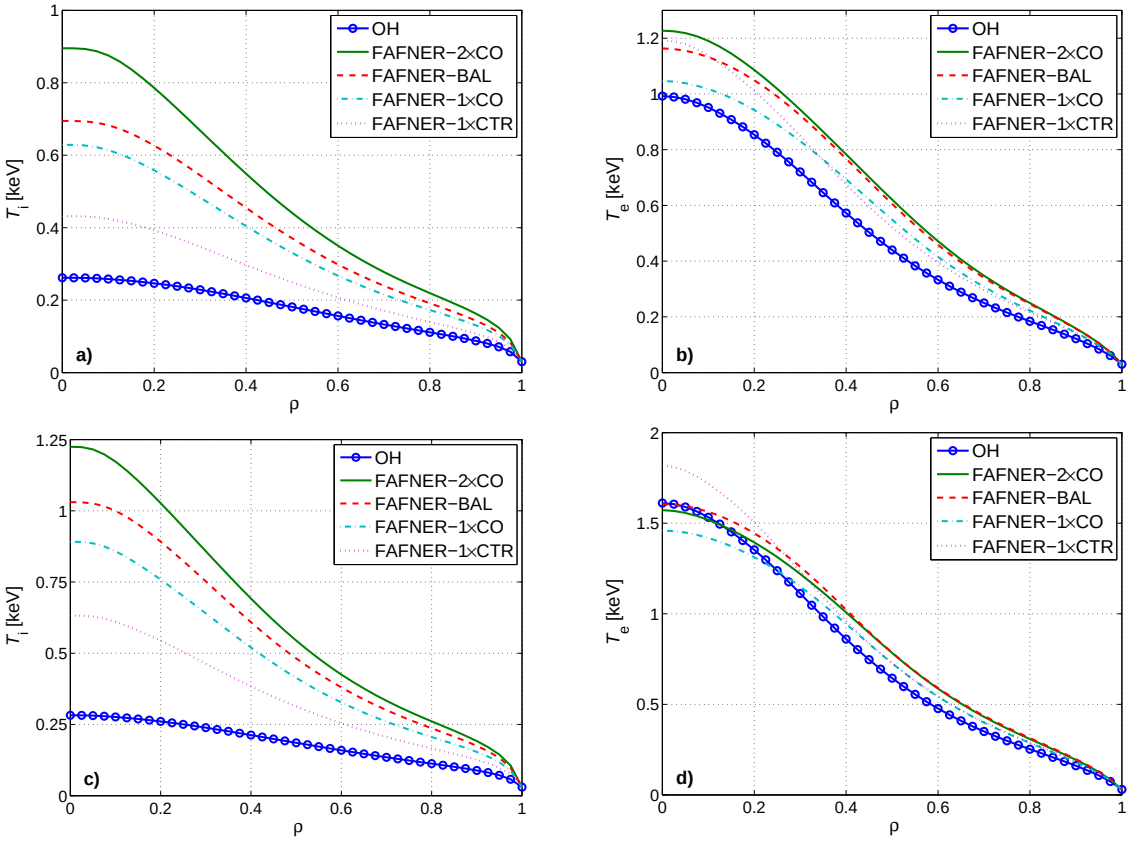

Figure 8. Temperature profiles from ASTRA simulations: (a) SND1 ion temperature, (b) SND1 electron temperature, (c) SND2 ion temperature, (d) SND2 electron temperature. Simulations include scenarios with dual co-injection, balanced injection, single co- and counter-injection calculated by FAFNER. Ohmic base case is also included for reference.

In Fig. 8, the reference ohmic cases are compared with on-axis NBI heated FAFNER

simulations in dual co-current injection, balanced (co+counter injection), single co-injection and single counter-injection scenarios in the SND1 and SND2 cases.

The central ion temperatures in the on-axis heating calculated by FAFNER by far exceed the ohmic values, in keeping with the intended goal for NBI heating. In the balanced configuration (i.e., co- + counter-injection) lower central ion temperatures are reached which can most likely be attributed to higher orbit losses associated with counter injection. Lower ion temperatures can also be seen in single counter-injection scenario compared to single co-injection one.

The electron temperature profiles suffer less change by the introduction of NBI heating. Interestingly enough in the single counter-injection mode, higher central electron temperatures are reached compared to the single co-injection mode; this can be attributed to higher central ohmic heating which results from the fact that the counter-injection drives central non-inductive current in the opposite direction causing the feedback system, which keeps the total plasma current constant, to increase the loop voltage and thereby central ohmic current. This effect is even more pronounced in the SND2 case where for certain injection modes, the ohmic-only heated discharges reach higher central electron temperatures. Outside the central region, the electron temperatures seem not to be affected by this and are proportional to the total absorbed power.

5. Conclusions

Self-consistently coupled codes ASTRA (transport) and FAFNER (NBI Fokker-Planck) have been successfully used for predictive simulations of the COMPASS operation at IPP Prague. The NBI performance is studied in detail. Major loss channels are identified, particularly the orbit-losses for counter-current injection and the beam-halo losses, which are pronounced for the full-power injection due to frequent charge-exchange collisions of fast NBI ions with slow beam-halo neutrals. The beam-halo losses are also an effect of the chosen 40 keV NBI energy. This energy is, however, shown to be optimum for COMPASS. Our simulations indicate that the NBI power will be centrally absorbed mainly by ions with relatively high power densities up to 10 MW/m^3. NBI can drive approximately $35 - 45$ kA of non-inductive current in the optimum dual co-injection configuration. If it were possible to decrease the NBI energy to 20 keV then radial injection could be exploited for diagnostic purposes.

The transport simulations with ASTRA-FAFNER carried out here have demonstrated that the NBI system described herein can significantly increase to around 1 keV the rather low ion temperatures $\sim$0.25 keV of the ohmically heated COMPASS plasma. In conclusion, the simulation results show that with the proposed 600 kW NBI, the ion temperatures can reach the desired keV range, far surpassing the few hundred eV values normally reached with only electron heating by ohmic, LH and ECRH schemes. Such ion temperatures are traditionally difficult to reach in smaller tokamaks.

Acknowledgments

This work has been partly supported by EURATOM, by EFDA, by the United Kingdom Engineering and Physical Sciences Research Council, by the Academy of Sciences of the Czech Republic project AV0Z-20430508, and by the research program "Research Center of Laser Plasma" LC528 of the Ministry of Education, Youth and Sport of the Czech Republic. FAFNER was kindly provided by Max-Planck-Institut für Plasmaphysik, Garching.

References

[1] Pánek R et al 2006 *Czechoslovak Journal of Physics* **56** B125-B37
[2] Tani K, Azumi M and Devoto R S 1992 *Journal of Computational Physics* **98** 332-41
[3] Fuchs V, Voitsekhovitch I, Bilyková O, Fitzgerald M, Pánek R, Urban J, Valovič M, Žáček F and Stöckel J 2006 *Europhysics Conference Abstracts* **30I** P1.103
[4] Bilyková O, Fuchs V, Pánek R, Urban J, Žáček F, Stöckel J, Voitsekhovitch I, Valovič M and Fitzgerald M 2006 *Czechoslovak Journal of Physics* **56** B24-B30
[5] Pereverzev G V and Yushmanov P N 2002 *ASTRA; Automated system for transport analysis* (IPP Report 5/98)
[6] Lister G G 1985 *FAFNER – A Fully 3-D Neutral Beam Injection Code Using Monte Carlo Methods* (IPP Report 4/222)
[7] Urban J, Fuchs V, Pánek R, Preinhaelter J, Stöckel J, Žáček F, Davydenko V I and Mishagin V V 2006 *Czechoslovak Journal of Physics* **56** B176-B81
[8] Fuchs V, Bilyková O, Pánek R, Stránský M, Stöckel J, Urban J and Žáček F 2008 *Europhysics Conference Abstracts* **32D** P2.098
[9] Succi S and Lister G G 1982 *3rd Joint Varenna-Grenoble Int. Symp. on Heating in Toroidal Plasmas* 137-42
[10] Speth E 1989 *Reports on Progress in Physics* **52** 57-121
[11] Erba M, Cherubini A, Parail V V, Springmann E and Taroni A 1997 *Plasma Physics and Controlled Fusion* **39** 261-76
[12] Valovič M, Fielding S J, Lloyd B, Manhood S J, Morris A W, Pinfold T, Stammers K and Warrick C D 1999 *Europhysics Conference Abstracts* **23J** P1.010
[13] Voitsekhovitch I, Litaudon X, Moreau D, Aniel T, Becoulet A, Erba M, Joffrin E, Kazarian-Vibert F and Peysson Y 1997 *Nuclear Fusion* **37** 1715-33
[14] Houlberg W A, Shaing K C, Hirshman S P and Zarnstorff M C 1997 *Physics of Plasmas* **4** 3230-42